J. Phycol. **46,** 1288–1295 (2010)

AN UNRECOGNIZED ANCIENT LINEAGE OF GREEN PLANTS PERSISTS IN DEEP MARINE WATERS[1]

Frederick W. Zechman[2,3]

Department of Biology, California State University Fresno, 2555 East San Ramon Ave, Fresno, California 93740, USA

Heroen Verbruggen,[3] *Frederik Leliaert*

Phycology Research Group, Ghent University, Krijgslaan 281 S8, 9000 Ghent, Belgium

Matt Ashworth

University Station MS A6700, 311 Biological Laboratories, University of Texas at Austin, Austin, Texas 78712, USA

Mark A. Buchheim

Department of Biological Science, University of Tulsa, Tulsa, Oklahoma 74104, USA

Marvin W. Fawley

School of Mathematical and Natural Sciences, University of Arkansas at Monticello, Monticello, Arkansas 71656, USA
Department of Biological Sciences, North Dakota State University, Fargo, North Dakota 58105, USA

Heather Spalding

Botany Department, University of Hawaii at Manoa, Honolulu, Hawaii 96822, USA

Curt M. Pueschel

Department of Biological Sciences, State University of New York at Binghamton, Binghamton, New York 13901, USA

Julie A. Buchheim, Bindhu Verghese

Department of Biological Science, University of Tulsa, Tulsa, Oklahoma 74104, USA

and M. Dennis Hanisak

Harbor Branch Oceanographic Institution, Fort Pierce, Florida 34946, USA

We provide molecular phylogenetic evidence that the obscure genera *Palmophyllum* Kütz. and *Verdigellas* D. L. Ballant. et J. N. Norris form a distinct and early diverging lineage of green algae. These palmelloid seaweeds generally persist in deep waters, where grazing pressure and competition for space are reduced. Their distinctness warrants recognition as a new order, the Palmophyllales. Although phylogenetic analyses of both the 18S rRNA gene and two chloroplast genes (*atp*B and *rbc*L) are in agreement with a deep-branching Palmophyllales, the genes are in conflict about its exact phylogenetic placement. Analysis of the nuclear ribosomal DNA allies the Palmophyllales with the prasinophyte genera *Prasinococcus* and *Prasinoderma* (Prasinococcales), while the plastid gene phylogeny placed *Palmophyllum* and *Verdigellas* as sister clade to all other Chlorophyta.

Key index words: **Chlorophyta; green algae; molecular phylogenetics; Palmophyllaceae fam. nov.; Palmophyllales ord. nov.; *Palmophyllum*; Prasinophyceae; *Verdigellas*; Viridiplantae**

Abbreviations: **AU, approximately unbiased; BI, Bayesian inference; ML, maximum likelihood; *PV*, *Palmophyllum-Verdigellas;* SH, Shimodaira–Hasegawa; UTC, Ulvophyceae-Trebouxiophyceae-Chlorophyceae**

Current hypotheses on the evolution of green plants (Viridiplantae) posit the early divergence of two discrete clades from an ancestral green flagellate unicell (Lewis and McCourt 2004). One clade, the Streptophyta, comprises the land plants and the charophytes. The other clade, the Chlorophyta, comprises the remainder of the green algae. Recent multimarker and genome-scale phylogenetic studies have sought to determine the origins of the land plants and have primarily focused on the green algal progenitors of the Streptophyta (Lemieux

[2]Author for correspondence: e-mail zechman@csufresno.edu.
[3]These authors contributed equally to this work.

et al. 2007, Rodríguez-Ezpeleta et al. 2007). In contrast, no multimarker assessments of the diversity and early evolution of the Chlorophyta have been undertaken. The 18S phylogenetic studies of Chlorophyta have identified the prasinophytes as a paraphyletic basal assemblage (Guillou et al. 2004), reinforcing the notion that the ancestral Chlorophyta were marine prasinophytes. Relationships among the prasinophyte lineages and the nature of the earliest diverging lineage of the Chlorophyta, however, remain poorly understood (Turmel et al. 2009).

The origin of the Viridiplantae is ancient—estimated to be from 500 to 1,500 million years before present (Yoon et al. 2004, Berney and Pawlowski 2006, Cavalier-Smith 2006). Such antiquity often confounds phylogenetic reconstruction of early diversifications due both to the lack of information in DNA sequence data and to methodological biases (Philippe et al. 2000). The massive amounts of information in genome-scale phylogenetic data sets have the potential to resolve ancient branching events, but, as yet, their contribution to understanding early divergences is limited by sparse taxon sampling. Accurate reconstruction of the earliest radiations of the green lineage will require a rich sampling both in terms of exemplar taxa and molecular markers.

Identification of early branching lineages is also crucial to mitigate the effects of methodological biases in phylogenetic reconstruction and to make robust inferences about the nature of the common ancestor of the green plant lineage. Contrary to expectations, environmental sequencing of marine picoplankton has not led to the discovery of major new green algal lineages (Guillou et al. 2004). Conversely, sampling of challenging habitats has revealed novel phylodiversity, as exemplified by studies of hypersaline, desert-soil, and Antarctic ecosystems (Lewin et al. 2000, Lewis and Lewis 2005, De Wever et al. 2009).

Marine, low-light, benthic ecosystems present another challenging environment for photosynthetic eukaryotes, and only a few algae live at the lower limits of the photic zone (Littler et al. 1985). *Palmophyllum*, *Verdigellas*, and *Palmoclathrus* Womersley comprise a group of green algae that thrive in deepwater and other dimly lit, benthic marine habitats (Womersley 1984, Nelson and Ryan 1986, Ballantine and Norris 1994, Ballantine and Aponte 1996). *Verdigellas* has mostly been recorded from depths >100 m, whereas *Palmophyllum* and *Palmoclathrus* species occur in somewhat shallower water, generally between 20 and 100 m. These seaweeds feature a unique type of multicellularity, forming firm, well-defined macroscopic thalli (Fig. 1, A and B) composed of isolated spherical cells in a gelatinous matrix (palmelloid thallus organization) (Fig. 1C). Although cells throughout the gelatinous matrix are morphologically and ultrastructurally identical, certain members have evolved relatively large, erect thalli with specialized gross morphological features. Individuals of the deepwater genus *Verdigellas* attach to substrate by means of one or more distinct holdfast structures (Fig. 1B), from which thalli expand above, yielding an umbrella-like morphology well adapted to maximally capture the sparse light penetrating from the sea surface and reflected from the underlying substratum. *Palmoclathrus*, a genus from seasonally changing temperate waters, features a stout, perennial holdfast system consisting of a basal disk and one to several cylindrical stalks from which seasonal peltate blades grow (Womersley 1984). Despite careful investigation (Nelson and Ryan 1986, O'Kelly 1988, Pueschel et al. 1997), motile stages and their accompanying basal bodies and flagellar roots have never been observed. The lack of evidence for these crucial ultrastructural features obscures the systematic position of these genera within the green algae. Even so, recent authors have attempted to classify them, variously placing them in the chlorophycean order Tetrasporales, the family Palmellaceae (Womersley 1984) or Palmellopsidaceae (Kraft 2007), or the order Chlorococcales (Abbott and Huisman 2004).

Our goal is to assess the affinities of *Palmophyllum* and *Verdigellas* by means of phylogenetic analysis of DNA sequence data of two large plastid-encoding genes (*atp*B and *rbc*L) and the nuclear-encoded 18S rRNA gene.

MATERIALS AND METHODS

DNA extraction and amplification. DNA extraction followed a modified cetyltrimethylammonium bromide (CTAB) extraction with the use of Phase Lock Gel (5 Prime Inc., Gaithersburg, MD, USA) during the first phenol/chloroform spin to separate DNA-containing aqueous phase from polysaccharide matrix. PCR and sequencing protocols followed Lam and Zechman (2006), with the exception that lower annealing temperatures (35°C) were used for the PCR amplification. New *atp*B (897 bp), *rbc*L (1,273 bp), and 18S (1,620 bp) sequences were generated for two *Palmophyllum* isolates, and new *rbc*L (514 bp) and 18S (1,394 bp) sequences were generated for *Verdigellas* (Table S1 in the supplementary material). *Palmophyllum* and *Verdigellas* specimens were deposited in the Bishop Museum Herbarium (BISH 730325, *Palmophyllum umbracola*), the Herbarium of the Museum of New Zealand (WELT A26526, *P. umbracola*), and the Harbor Branch Oceanographic Institute Herbarium (HBFH 7821 and 7822, *Verdigellas peltata*).

Alignment creation. For the 52 selected ingroup and additional outgroup taxa, DNA sequence data sets of two plastid genes (*rbc*L and *atp*B) and 18S nrDNA were assembled (Table S1). The *rbc*L and *atp*B data sets were based on ClustalW (Larkin et al. 2007) alignments of their corresponding amino acid sequences, and were respectively 1,386 and 1,380 bases long. The 18S sequences were manually aligned based on a comparative analysis of RNA secondary structure as described in Cocquyt et al. (2009), resulting in an alignment of 2,000 bases. Two alignments were created for phylogenetic analysis: the plastid data set (concatenated *atp*B and *rbc*L sequences) and the nuclear (18S) data set. We did not concatenate 18S with the plastid genes because phylogenetic analyses indicated conflict between these data sets (see Results). Alignments are available through TreeBase (http://www.treebase.org).

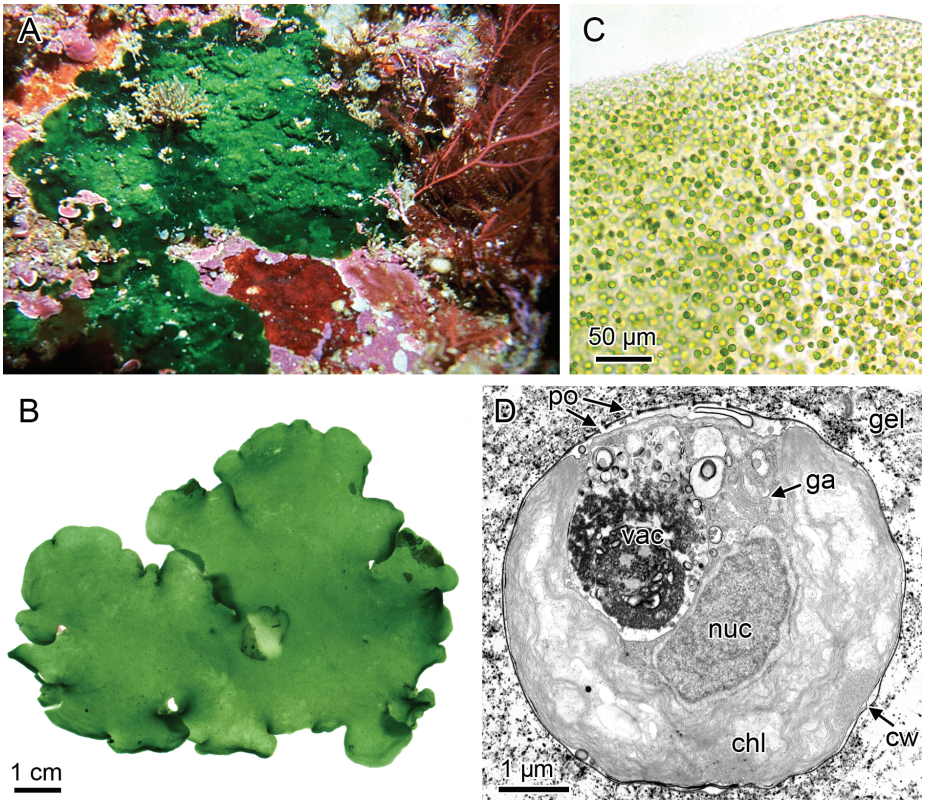

FIG. 1. External appearance, anatomy, and ultrastructure of the genera *Palmophyllum* and *Verdigellas*. (A) *Palmophyllum*, whose crustose thalli are tightly adherent to the substrate, is shown growing on a reef in New Zealand. (B) *Verdigellas peltata*, a species growing in low-light habitats (~100–200 m) in the western Atlantic Ocean, is attached to the substrate by a central holdfast disk and, in older specimens, secondary points of attachment. (C) Cross-section of *Palmophyllum* thallus, composed of coccoid cells embedded in a gelatinous matrix. (D) TEM image of a single *Verdigellas* cell (5.5 μm in diameter) with a single cup-shaped chloroplast (chl) surrounding a cytoplasmic pocket containing the nucleus (nuc) and a large vacuole (vac) with lamellar material (dark). Pores (po) in the cell wall (cw) above the cytoplasmic pocket facilitate export of gelatinous material (gel) from Golgi-derived vesicles (ga). Photograph in (A) by L. D. Ritchie, Northland, New Zealand.

Partitioning strategy, model choice, and phylogenetic analyses. Partitioning strategy and model selection followed the methodologies described in Verbruggen and Theriot (2008) and are detailed in Appendix S1 in the supplementary material.

The alignments were analyzed using Bayesian inference (BI) and maximum likelihood (ML) phylogenetic methods. The 18S alignment was partitioned into stems and loops, and a general time reversible (GTR)+Γ_8 model was applied to each partition. The plastid data were partitioned into codon positions, with a GTR+Γ_8 model for each. BI was carried out in MrBayes v.3.1.2 (Ronquist and Huelsenbeck 2003). Two runs of four chains each were run in parallel for 5 million generations, applying the default priors. Convergence of the log-likelihood and model parameters was visually checked in Tracer v. 1.4 (Rambaut and Drummond 2007). Burn-in was set at 3 million generations, well beyond the point of convergence of all analyses. ML analyses were carried out with TreeFinder, which allows likelihood tree searches under partitioned models (Jobb et al. 2004). Tree space coverage in the TreeFinder program is low compared to other ML programs. Therefore, independent tree searches were run from different starting trees. The starting trees were produced by randomly modifying the guide tree used for model selection by a number of nearest neighbor interchange (NNI) steps. The departure from the guide tree was 100 and 200 NNI steps (50 replicates each). ML tree searches started from each of the resulting trees and used the same partitions and models as the BI. The second-level tree search was used, and partition rates were optimized under the proportional model. Branch support was calculated using the bootstrap resampling method (1,000 pseudoreplicates) (Felsenstein 1985). Bootstrap analyses used the same settings but started from the ML tree. The glaucocystophyte *Cyanophora paradoxa* was used as outgroup taxon for the plastid gene analysis; the reason why we did not use a red alga as outgroup is that this group has acquired the *rbc*L gene by lateral gene transfer (Delwiche and Palmer 1996). For the 18S analysis, *C. paradoxa*, the cyanidiophyte *Cyanidioschyzon merolae,* and the red alga *Porphyra yezoense* were used as outgroups.

Supplementary phylogenetic analyses were performed to evaluate the effect of outgroup selection, removal of fast-evolving sites, alignment method, partitioning strategy, and model selection on tree topology and branch support (see Appendix S2 in the supplementary material).

Topological conflict. To assess the significance of some conflicting relationships observed in the 18S and plastid trees, Shimodaira–Hasegawa (SH) and approximately unbiased (AU) tests were carried out (Shimodaira and Hasegawa 1999, Shimodaira 2002). Three hypothesis derived from the plastid phylogeny were constrained on the 18S data and compared to the original 18S tree (Fig. 3, A–C). Three hypotheses derived from the 18S phylogeny were constrained on the plastid data and compared to the original plastid tree (Fig. 3, D–F). The six

hypotheses were coded as constraints in MrBayes, and constrained analyses were run with the same parameter settings as the original analyses. Site-specific likelihoods were calculated for the unconstrained and constrained Bayesian trees using PAML v. 4 (Yang 2007), with the same partitions and models used in the original analyses, but with model parameters optimized by baseml. Significance testing (SH and AU) was carried out using CONSEL v. 1.19 (Shimodaira and Hasegawa 2001).

RESULTS

Our phylogenetic results indicate that *Palmophyllum* and *Verdigellas* (*PV*) comprise a distinct, highly divergent, and strongly supported lineage of green algae (Fig. 2), yet analyses of the 18S and plastid gene alignments resulted in two different tree topologies. The plastid gene phylogeny (Fig. 2A) recovered the *PV* clade as sister to all other Chlorophyta with moderate support (BI posterior probability = 0.97, ML bootstrap proportion = 77). In contrast, the 18S alignment recovered three major lineages, the relationships among which were not resolved (Fig. 2B). One lineage is composed of the *PV* clade and two coccoid prasinophyte genera, *Prasinococcus* and *Prasinoderma* (Prasinococcales). The second and third lineages are the Streptophyta and a clade formed by the remaining prasinophytes and UTC (Ulvophyceae-Trebouxiophyceae-Chlorophyceae) taxa. Thus, according to the 18S data, prasinophytes represent a nonmonophyletic assemblage that has given rise to the *PV* clade and the UTC clade, while the plastid phylogeny recovers the prasinophytes as monophyletic (except for the genus *Tetraselmis*).

Analyses with alternative outgroup combinations, removal of rapidly evolving sites, and less complex partitioning strategies yielded virtually identical results (Appendix S2). Trees inferred from the 18S data set, aligned using secondary structure information or aligned automatically using MUSCLE (Edgar 2004), were congruent in placing *PV*, *Prasinococcus,* and *Prasinoderma* in a single clade. The analysis of the 18S data set with *Cyanophora* as the only

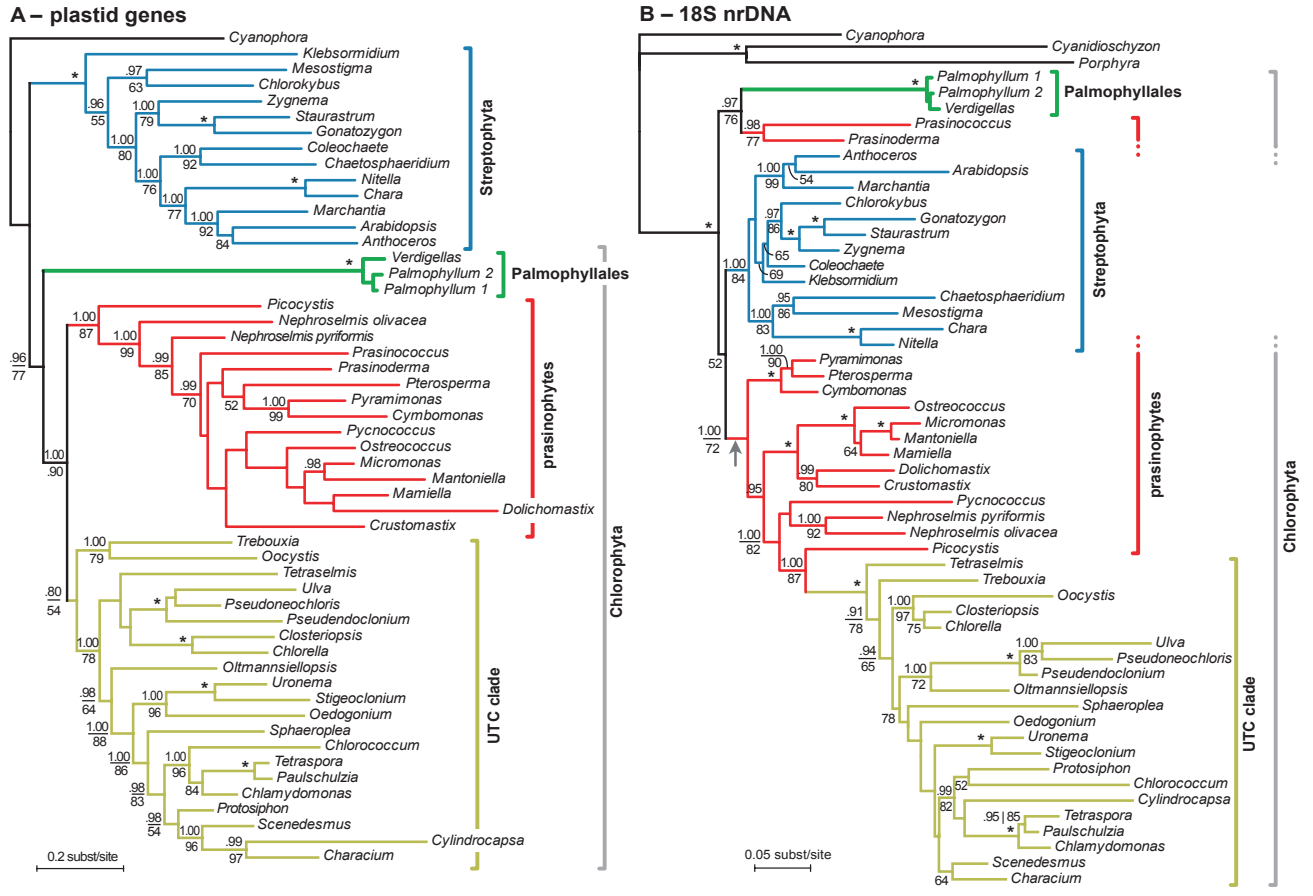

FIG. 2. Bayesian majority rule trees showing all compatible partitions, inference from the plastid genes (A) and 18S nrDNA (B). The plastid data were partitioned into codon positions, with a GTR+Γ_8 model applied to each partition. The 18S alignment was partitioned into stems and loops with a GTR+Γ_8 model applied to each partition. Node support is given as Bayesian posterior probabilities (above branches) and maximum-likelihood (ML) bootstrap values (below branches); values <0.9 and 50, respectively, are not shown; the nodes that received full support are denoted by an asterisk. The Palmophyllales are highlighted by a green, boldface branch; the arrow indicates the position of the Palmophyllales-*Prasinococcus*-*Prasinoderma* clade in some of the 18S phylogenetic analyses (see Fig. S5 in Appendix S2 of the supplementary material). GTR, general time reversible.

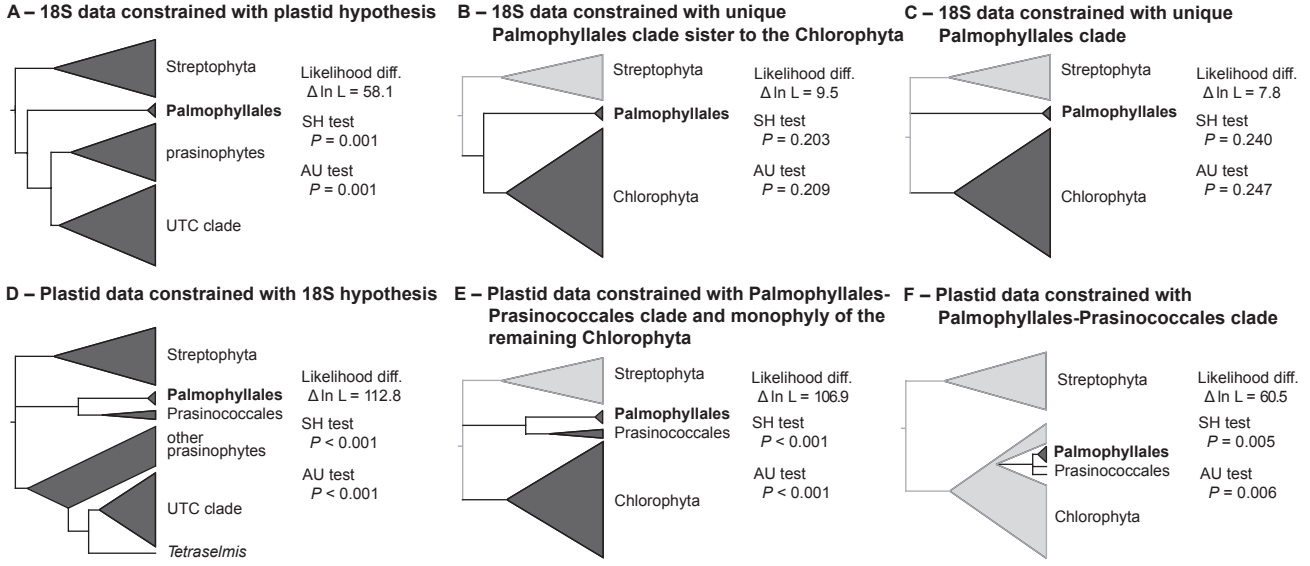

FIG. 3. Comparing alternative hypotheses using the SH and AU tests. The topological schemas (hypotheses) are derived from the trees in Figure 2. In panels (A–C), the hypothesis derived from the plastid phylogeny was constrained on the 18S data and compared to the original 18S tree. These constraints include (A) monophyletic prasinophytes (including Prasinococcales) sister to the UTC clade, a unique Palmophyllales clade sister to the Chlorophyta, and Streptophyta sister to the Palmophyllales-Chlorophyta clade; (B) a unique Palmophyllales clade (i.e., unrelated to Prasinococcales) sister to the Chlorophyta; (C) a unique Palmophyllales clade only. In panels (D–F), the hypothesis derived from the 18S phylogeny was constrained on the plastid data and compared to the original plastid tree. These constraints include (D) a sister relation between the Palmophyllales and the Prasinococcales, a sister relation between *Tetraselmis* and the UTC clade, and monophyly of the Chlorophyta (excluding Palmophyllales and Prasinococcales); (E) monophyly of Palmophyllales-Prasinococcales, and monophyly of the rest of the Chlorophyta; and (F) monophyly of Palmophyllales-Prasinococcales only (this clade was automatically placed among the prasinophytes by the constrained Bayesian analysis). AU, approximately unbiased; SH, Shimodaira–Hasegawa; UTC, Ulvophyceae-Trebouxiophyceae-Chlorophyceae.

outgroup, and the analyses excluding fast-evolving regions, differ from the tree shown in Figure 2B in that they recover the *PV*-Prasinococcales clade as sister to the remaining Chlorophyta (Appendix S2). However, support for this association is low (posterior probabilities < 0.79), reinforcing the notion of three main lineages with uncertain branching order.

A graphical representation of the topological differences between the plastid and 18S trees is given in Figure 3. The tree inferred from the 18S data set constrained to conform to the plastid hypothesis had a significantly lower likelihood than the original 18S tree (Fig. 3A). However, trees constrained only with a unique *PV* clade sister to the Chlorophyta or only with a unique *PV* clade could not be rejected by the 18S data (Fig. 2, B and C). The tree inferred from the plastid data set constrained to conform to the 18S hypothesis had a significantly lower likelihood than the original tree (Fig. 3D). More specifically, trees only constrained with a sister relation between the *PV* clade and the Prasinococcales were significantly rejected by the plastid data (Fig. 3, E and F). In other words, the plastid data seem to contain a strong signal in support of a unique *PV* lineage, whereas the 18S data are less robust in support of a *PV*-Prasinococcales relationship. Overall, each data set appears to contain a clear phylogenetic signal that conflicts with the phylogenetic signal in the other data set.

DISCUSSION

Our data provide evidence that the genera *Palmophyllum* and *Verdigellas* form a distinct and early diverging lineage of green algae. The highly divergent nature of these genera warrants their recognition as a discrete group at the order level.

Palmophyllales Zechman, Verbruggen, Leliaert, Ashworth, M. A. Buchheim, Fawley, H. Spalding, Pueschel, J. A. Buchheim, Verghese et Hanisak ord. nov.

Algae benthicae marinae. Thallus viridis vel atroviridis, cum textura gelatinosa firma. Thallus macroscopicus, crustosus vel erectus. Thallus cellulis subsphaericis in matrice gelatinosa compositus. Cellulae in matrice solida gelatinosa irregulariter sed saepius prope superficiem dispositae. Cellularum diameter 6–10 μm. Cellulae cum chloroplasto unico cupulato sine pyrenoidibus.

Benthic marine algae. Thallus green to deep green, of firm gelatinous texture. Thallus macroscopic, crustose or erect. Thallus composed of subspherical cells in gelatinous matrix. Cells irregularly distributed throughout the whole gelatinous matrix but more frequent near surface. Cell diameter 6–10 μm. Cells with a single cup-shaped chloroplast without pyrenoids.

Palmophyllaceae Zechman, Verbruggen, Leliaert, Ashworth, M. A. Buchheim, Fawley, H. Spalding, Pueschel, J. A. Buchheim, Verghese et Hanisak fam. nov.: Cum characteribus ordo. Characters as for order.

Genera *Palmophyllum* (type), *Verdigellas*.

The relatedness between *Palmophyllum*, *Verdigellas,* and *Palmoclathrus* had already been hypothesized on the basis of microscopic and ultrastructural features (Ballantine and Norris 1994, Pueschel et al. 1997). The close relationship between *Palmophyllum* and *Verdigellas* is now confirmed by molecular evidence. No sequence data are currently available for *Palmoclathrus*.

The classification of *Palmophyllum*, *Verdigellas*, and *Palmoclathrus* among other green algae has been debated. Motile stages, which contain basal bodies and flagellar roots that serve as the principal characters underlying the classification of the Chlorophyta, have not been observed in any species of the three genera (Nelson and Ryan 1986, Pueschel et al. 1997). The absence of these crucial ultrastructural characters has forced a reliance on gross morphological traits that are prone to convergence. Earlier studies assigned the three genera to the chlorophycean orders Chlorococcales (Nelson and Ryan 1986, O'Kelly 1988), whose members feature a similar pattern of cell division, or Tetrasporales (families Palmellaceae or Palmellopsidaceae) (Ballantine and Norris 1994), with which the three genera share a palmelloid organization (i.e., small spherical cells embedded in mucilage). Both hypotheses are rejected by our molecular results, indicating that the characters used to infer these relationships have evolved independently in the respective lineages. In the taxonomic treatise by Silva (1982), the genera *Palmophyllum*, *Verdigellas,* and *Palmoclathrus* were included in the tetrasporalean family Palmellopsidaceae, but the author remarked that information essential to the confirmation of this placement is lacking and that the genera probably constitute a distinct family. Our phylogenetic results indicate that the *PV* clade deserves recognition at a higher taxonomic rank, hence their description as a new order. The different signal about the phylogenetic position of the Palmophyllales in the 18S and plastid data hampers the placement of the order into one of the classes of recent chlorophytan classification schemes (Marin and Melkonian 2010). For now, we recognize the Palmophyllales as an order within the Prasinophyceae sensu lato (Moestrup and Throndsen 1988).

Our analyses of the 18S data suggest a sister relationship of the Palmophyllales and the coccoid genera *Prasinoderma* and *Prasinococcus* (Prasinococcales), which have been shown to form an early diverging prasinophyte lineage (Gescher et al. 2008, Turmel et al. 2009). Several cytological similarities between these taxa can be identified, none of which, however, is unique to the alliance. Cell size (<10 μm), cell wall structure during the stationary phase, the cell division mechanism, and the absence of flagella and centrioles in the main vegetative stage comprise these nonapomorphic similarities. Cytokinesis in *Prasinoderma* is very similar to that described in *Palmoclathrus*, both being characterized by asymmetrical binary cell division in which one daughter cell is released while the other retains the parent wall (O'Kelly 1988, p. 250, figs. 3–11; Hasegawa et al. 1996, pp. 174–5, figs. 10–26; Jouenne et al., in press). A similar cell division mechanism has also been described in the unrelated prasinophyte *Pycnococcus*. The overall arrangement of organelles is also similar, but this may simply be due to the spatial constraint of a cup-shaped chloroplast surrounding a cytoplasmic pocket (Fig. 1D). *Verdigellas* and *Prasinococcus* also have what has been interpreted to be a mucus-secreting system, consisting of an elaborate Golgi body and a set of pores through the cell wall adjacent to the cytoplasmic pocket (Pueschel et al. 1997, Sieburth et al. 1999). Despite the similarities in this system, the pores of *Verdigellas* (Pueschel et al. 1997) are much simpler in structure than the Golgi-decapore complex of *Prasinococcus* (Sieburth et al. 1999). Thus, the only indication of pore homology is in the context of the 18S phylogenetic result, and it is clear that homology of such functional adaptations should not be assumed without further study. Interestingly, the cells of *Prasinoderma singularis* are sometimes surrounded by a mucus-like secretion (Jouenne et al., in press). Although it is interesting to speculate on potential synapomorphies for the Palmophyllales and Prasinococcales, the topology obtained with plastid data does not lead to such inferences. However, given that a paraphyletic branching pattern of prasinophytes has been demonstrated by several molecular phylogenetic studies of both single genes and complete plastid genomes (e.g., Turmel et al. 2009, Marin and Melkonian 2010), the prasinophyte relationships in the present plastid phylogeny are probably an artifact related to insufficient phylogenetic information in the two plastid genes and the missing *atp*B data for most prasinophytes.

It is striking that an ancient lineage of green algae such as the Palmophyllales almost exclusively occurs in dimly lit deepwater habitats. Phylogenetic relicts of several other groups of organisms also persist in deepwater habitats. For example, the continental slopes are home to ancient lineages such as the hagfishes (Jorgensen et al. 1997), chimaeras and cow sharks (Weitzman 1997), and stalked crinoids and other ancient invertebrate lineages (Briggs 1974). The onshore-offshore hypothesis describes the onshore origination and offshore retreat of marine organismal groups in the fossil record (Jablonski et al. 1983, Bottjer and Jablonski 1988). The onshore-offshore hypothesis has been cited in relation to the ecological diversification of coralline red algae (Aguirre et al. 2000). The early branching position of the taxon-poor, deepwater Palmophyllales compared to the taxon-rich and predominantly shallow-water prasinophytes and UTC taxa may be interpreted as another instance of photosynthetic organisms supporting this hypothesis. The minimum light requirement for photosynthesis is an

important determinant of the depth distribution of algal species and explains the paucity of algae on the continental slope. Only 0.05% of the irradiance at the surface (PAR) penetrates to the continental shelf habitats where *Verdigellas* typically occurs (Littler et al. 1985), and its primary productivity is a mere fraction of that of shallow-water green algae (Littler et al. 1986). *Palmophyllum* lacks the green light-harvesting photosynthetic pigments siphonoxanthin and siphonein typically found in other low-light-adapted green algae (Nelson and Ryan 1986, Sartoni et al. 1993). Instead, the genus seems to have adapted to low-light conditions by maintaining increased chl *b/a* ratios (Hooks et al. 1988, Sartoni et al. 1993).

The ability to grow in deep habitats with low, attenuated light conditions may be of key importance to the persistence of these algae. Deep habitats feature diminished abiotic stressors (e.g., wave action, temperature variation) and lower levels of competition for substrata. Herbivores also decline sharply with increasing depth, both in abundance and species richness (Thresher and Colin 1986, Brokovich et al. 2008). Unlike entities derived from younger green algal radiations, especially those in the UTC lineage, whose morphological and biochemical adaptations allow them to withstand such stresses (Duffy and Hay 1990), *Verdigellas* is readily consumed by common shallow-water herbivores in feeding experiments (M. Littler and D. Littler, personal communication). The deepwater habitats likely provide *Palmophyllum*, *Verdigellas,* and *Palmoclathrus* with an ecological refuge in which they experience reduced competition and herbivory.

In conclusion, *Palmophyllum* and *Verdigellas* form a distinct and ancient lineage of green algae, and it is clear that this group requires more attention, from a morphological, ecological, and evolutionary perspective. It is generally accepted that the ancestor of the Viridiplantae was a unicellular flagellate organism. The deep phylogenetic position of a lineage of palmelloid green algae may have implications for our understanding of the early morphological evolution of green algae. Additional multilocus phylogenetic analyses, including plastid phylogenomics, will be required to elucidate the exact phylogenetic position of the Palmophyllales.

We are grateful to Wendy Nelson for providing *Palmophyllum* samples and a photograph by L. D. Ritchie (Fig. 1A). We thank Debashish Bhattacharya, Olivier De Clerck, Charles Delwiche, Michael Donoghue, Paul Goetghebeur, Rick McCourt, Brent Mishler, John Morrissey, and Fabio Rindi for insightful comments on previous versions of the manuscript. Analyses were carried out on the KERMIT computing cluster (Ghent University). We thank Wim Gillis for technical support. This work was supported by grants from the National Science Foundation (#0128977 to F. W. Z., #0129030 to M. A. B., #0128952 to M. W. F.), the Research Foundation – Flanders (postdoctoral fellowships to H. V. and F. L.), and the Ghent University Special Research Fund (visiting scholar grant to F. W. Z.). This manuscript is Contribution #1813 from Harbor Branch Oceanographic Institute at Florida Atlantic University.

Abbott, I. A. & Huisman, J. M. 2004. *Marine Green and Brown Algae of the Hawaiian Islands*. Bishop Museum Press, Honolulu, Hawaii, 259 pp.

Aguirre, J., Riding, R. & Braga, J. C. 2000. Diversity of coralline red algae: origination and extinction patterns from the Early Cretaceous to the Pleistocene. *Paleobiology* 26:651–67.

Ballantine, D. L. & Aponte, N. E. 1996. *Verdigellas nektongammea* (Tetrasporales, Chlorophyta), a new deep-water species from the Bahamas. *Nova Hedwigia* 62:425–9.

Ballantine, D. L. & Norris, J. N. 1994. *Verdigellas*, a new deep-water genus (Tetrasporales, Chlorophyta) from the tropical western Atlantic. *Cryptogam. Bot.* 4:368–72.

Berney, C. & Pawlowski, J. 2006. A molecular time-scale for eukaryote evolution recalibrated with the continuous microfossil record. *Proc. R. Soc. B Biol. Sci.* 273:1867–72.

Bottjer, D. J. & Jablonski, D. 1988. Paleoenvironmental patterns in the evolution of post-Paleozoic benthic marine invertebrates. *Palaios* 3:540–60.

Briggs, J. C. 1974. *Marine Zoogeography*. McGraw-Hill, New York, 475 pp.

Brokovich, E., Einbinder, S., Shashar, N., Kiflawi, M. & Kark, S. 2008. Descending to the twilight-zone: changes in coral reef fish assemblages along a depth gradient down to 65 m. *Mar. Ecol. Prog. Ser.* 371:253–62.

Cavalier-Smith, T. 2006. Cell evolution and earth history: stasis and revolution. *Philos. Trans. R. Soc. Lond. B Biol. Sci.* 361:969–1006.

Cocquyt, E., Verbruggen, H., Leliaert, F., Zechman, F., Sabbe, K. & De Clerck, O. 2009. Gain and loss of elongation factor genes in green algae. *BMC Evol. Biol.* 9:39.

De Wever, A., Leliaert, F., Verleyen, E., Vanormelingen, P., Van der Gucht, K., Hodgson, D. A., Sabbe, K. & Vyverman, W. 2009. Hidden levels of phylodiversity in Antarctic green algae: further evidence for the existence of glacial refugia. *Proc. R. Soc. B Biol. Sci.* 276:3591–9.

Delwiche, C. F. & Palmer, J. D. 1996. Rampant horizontal transfer and duplication of rubisco genes in eubacteria and plastids. *Mol. Biol. Evol.* 13:873–82.

Duffy, J. E. & Hay, M. E. 1990. Seaweed adaptations to herbivory. *Bioscience* 40:368–75.

Edgar, R. C. 2004. MUSCLE: a multiple sequence alignment method with reduced time and space complexity. *BMC Bioinformatics* 5:1–19.

Felsenstein, J. 1985. Confidence-limits on phylogenies: an approach using the bootstrap. *Evolution* 39:783–91.

Gescher, C., Metfies, K., Frickenhaus, S., Knefelkamp, B., Wiltshire, K. H. & Medlin, L. K. 2008. Feasibility of assessing the community composition of prasinophytes at the Helgoland roads sampling site with a DNA microarray. *Appl. Environ. Microbiol.* 74:5305–16.

Guillou, L., Eikrem, W., Chretiennot-Dinet, M. J., Le Gall, F., Massana, R., Romari, K., Pedros-Alio, C. & Vaulot, D. 2004. Diversity of picoplanktonic prasinophytes assessed by direct nuclear SSU rDNA sequencing of environmental samples and novel isolates retrieved from oceanic and coastal marine ecosystems. *Protist* 155:193–214.

Hasegawa, T., Miyashita, H., Kawachi, M., Ikemoto, H., Kurano, N., Miyachi, S. & Chihara, M. 1996. *Prasinoderma coloniale* gen. et sp. nov., a new pelagic coccoid prasinophyte from the western Pacific Ocean. *Phycologia* 35:170–6.

Hooks, C. E., Bidigare, R. R., Keller, M. D. & Guillard, R. R. L. 1988. Coccoid eukaryotic marine ultraplankters with four different HPLC pigment signatures. *J. Phycol.* 24:571–80.

Jablonski, D., Sepkoski, J. J., Bottjer, D. J. & Sheehan, P. M. 1983. Onshore-offshore patterns in the evolution of Phanerozoic shelf communities. *Science* 222:1123–5.

Jobb, G., von Haeseler, A. & Strimmer, K. 2004. TREEFINDER: a powerful graphical analysis environment for molecular phylogenetics. *BMC Evol. Biol.* 4:18.

Jorgensen, J. M., Lomholt, J. P., Weber, R. E. & Malte, H. 1997. *The Biology of Hagfishes*. Chapman & Hall, London, 578 pp.

Jouenne, F., Eikrem, W., Le Gall, F., Marie, D., Johnsen, G. & Vaulot, D. In press. *Prasinoderma singularis* sp. nov. (Prasinophyceae, Chlorophyta), a solitary coccoid prasinophyte from the south-east Pacific Ocean. *Protist*.

Kraft, G. T. 2007. *Algae of Australia: Marine Benthic Algae of Lord Howe Island and the Southern Great Barrier Reef. 1. Green Algae*. CSIRO Publishing, Melbourne, Australia, 347 pp.

Lam, D. W. & Zechman, F. W. 2006. Phylogenetic analyses of the Bryopsidales (Ulvophyceae, Chlorophyta) based on RUBISCO large subunit gene sequences. *J. Phycol.* 42:669–78.

Larkin, M. A., Blackshields, G., Brown, N. P., Chenna, R., McGettigan, P. A., McWilliam, H., Valentin, F., et al. 2007. Clustal W and Clustal X version 2.0. *Bioinformatics* 23:2947–8.

Lemieux, C., Otis, C. & Turmel, M. 2007. A clade uniting the green algae *Mesostigma viride* and *Chlorokybus atmophyticus* represents the deepest branch of the Streptophyta in chloroplast genome-based phylogenies. *BMC Biol.* 5:2.

Lewin, R. A., Krienitz, L., Goericke, R., Takeda, H. & Hepperle, D. 2000. *Picocystis salinarum* gen. et sp. nov. (Chlorophyta) – a new picoplanktonic green alga. *Phycologia* 39:560–5.

Lewis, L. A. & Lewis, P. O. 2005. Unearthing the molecular phylodiversity of desert soil green algae (Chlorophyta). *Syst. Biol.* 54:936–47.

Lewis, L. A. & McCourt, R. M. 2004. Green algae and the origin of land plants. *Am. J. Bot.* 91:1535–56.

Littler, M. M., Littler, D. S., Blair, S. M. & Norris, J. N. 1985. Deepest known plant life discovered on an uncharted seamount. *Science* 227:57–9.

Littler, M. M., Littler, D. S., Blair, S. M. & Norris, J. N. 1986. Deep-water plant communities from an uncharted seamount off San Salvador Island, Bahamas: distribution, abundance, and primary productivity. *Deep-Sea Res. Part I Oceanogr. Res. Pap.* 33:881–92.

Marin, B. & Melkonian, M. 2010. Molecular phylogeny and classification of the Mamiellophyceae class. nov. (Chlorophyta) based on sequence comparisons of the nuclear- and plastid-encoded rRNA operons. *Protist* 161:304–36.

Moestrup, Ø. & Throndsen, J. 1988. Light and electron microscopical studies on *Pseudoscourfieldia marina*, a primitive scaly green flagellate (Prasinophyceae) with posterior flagella. *Can. J. Bot.* 66:1415–34.

Nelson, W. A. & Ryan, K. G. 1986. *Palmophyllum umbracola* sp. nov. (Chlorophyta) from offshore islands of northern New Zealand. *Phycologia* 25:168–77.

O'Kelly, C. J. 1988. Division of *Palmoclathrus stipitatus* (Chlorophyta) vegetative cells. *Phycologia* 27:248–53.

Philippe, H., Lopez, P., Brinkmann, H., Budin, K., Germot, A., Laurent, J., Moreira, D., Muller, M. & Le Guyader, H. 2000. Early-branching or fast-evolving eukaryotes? An answer based on slowly evolving positions *Proc. R. Soc. B Biol. Sci.* 267:1213–21.

Pueschel, C., Sullivan, K. & Ballantine, D. 1997. Ultrastructure of *Verdigellas peltata* (Palmellaceae, Chlorophyta), a deep-water, palmelloid alga with ferritin and trilaminar sheaths. *Phycologia* 36:492–9.

Rambaut, A. & Drummond, A. J. 2007. *Tracer*. http://beast.bio.ed.ac.uk/tracer (accessed on March 22, 2010).

Rodríguez-Ezpeleta, N., Philippe, H., Brinkmann, H., Becker, B. & Melkonian, M. 2007. Phylogenetic analyses of nuclear, mitochondrial, and plastid multigene data sets support the placement of *Mesostigma* in the Streptophyta. *Mol. Biol. Evol.* 24:723–31.

Ronquist, F. & Huelsenbeck, J. P. 2003. MrBayes 3: Bayesian phylogenetic inference under mixed models. *Bioinformatics* 19:1572–4.

Sartoni, G., Cinelli, F., Hirata, T., Katayama, N. & Yokohama, Y. 1993. On the lack of green light-harvesting pigments and the extremely high chlorophyll b/a ratio in the deep-water green alga, *Palmophyllum crassum* (Chlorosphaerales). *Jpn. J. Phycol.* 41:327–31.

Shimodaira, H. 2002. An approximately unbiased test of phylogenetic tree selection. *Syst. Biol.* 51:492–508.

Shimodaira, H. & Hasegawa, M. 1999. Multiple comparisons of log-likelihoods with applications to phylogenetic inference. *Mol. Biol. Evol.* 16:1114–6.

Shimodaira, H. & Hasegawa, M. 2001. CONSEL: for assessing the confidence of phylogenetic tree selection. *Bioinformatics* 17:1246–7.

Sieburth, J. M., Keller, M. D., Johnson, P. W. & Myklestad, S. M. 1999. Widespread occurrence of the oceanic ultraplankter, *Prasinococcus capsulatus* (Prasinophyceae), the diagnostic ''Golgi-decapore complex'' and the newly described polysaccharide ''capsulan.'' *J. Phycol.* 35:1032–43.

Silva, P. C. 1982. Chlorophyceae. *In* Parker, S. P. [Ed.] *Synopsis and Classification of Living Organisms*. McGraw-Hill, New York, pp. 133–61.

Thresher, R. E. & Colin, P. L. 1986. Trophic structure, diversity and abundance of fishes of the deep reef (30–300 m) at Enewetak, Marshall-Islands. *Bull. Mar. Sci.* 38:253–72.

Turmel, M., Gagnon, M.-C., O'Kelly, C. J., Otis, C. & Lemieux, C. 2009. The chloroplast genomes of the green algae *Pyramimonas*, *Monomastix*, and *Pycnococcus* shed new light on the evolutionary history of prasinophytes and the origin of the secondary chloroplasts of euglenids. *Mol. Biol. Evol.* 26: 631–48.

Verbruggen, H. & Theriot, E. C. 2008. Building trees of algae: some advances in phylogenetic and evolutionary analysis. *Eur. J. Phycol.* 43:229–52.

Weitzman, S. H. 1997. Systematics of deep-sea fishes. *In* Randall, D. J. & Farrell, A. P. [Eds.] *Deep-Sea Fishes*. Academic Press, San Diego, California, pp. 43–77.

Womersley, H. B. S. 1984. *The Marine Benthic Flora of Southern Australia. Part I*. Government Printer, Adelaide, South Australia, 329 pp.

Yang, Z. 2007. PAML 4: phylogenetic analysis by maximum likelihood. *Mol. Biol. Evol.* 24:1586–91.

Yoon, H. S., Hackett, J. D., Ciniglia, C., Pinto, G. & Bhattacharya, D. 2004. A molecular timeline for the origin of photosynthetic eukaryotes. *Mol. Biol. Evol.* 21:809–18.

Supplementary Material

The following supplementary material is available for this article:

Appendix S1. Partitioning strategy and model choice.

Appendix S2. Supplementary phylogenetic analyses.

Table S1. List of taxa used in this study, with GenBank accession numbers of their *atp*B and *rbc*L and 18S nrDNA sequences. In some cases, genes from different species of the same genus were concatenated if the monophyly of the genus had been clearly demonstrated. New sequences are indicated in bold.

Appendix S1. Partitioning strategy and model choice.

Base frequencies and evolutionary rates were calculated to guide data partitioning. They were calculated for each gene and for different codon positions within each gene. Base frequencies were calculated with PAUP version 4.0b10 (Swofford 2003). Site-specific substitution rates were calculated under a Jukes-Cantor model with HyPhy (Kosakovsky Pond et al. 2005). The guide tree used for rate calculations and model selection was inferred with PhyML (Guindon and Gascuel 2003) using a JC69+Γ_4 model. Marked differences in base frequencies and substitution rates were found between codon positions (Figs. S1, S2). Because the rate and base frequency differences between codon positions were similar for *rbc*L and *atp*B, the plastid data were not partitioned into genes but into codon positions only. The advantages of partitioning into codon positions rather than genes in such circumstances have already been demonstrated (Brandley et al. 2005, Verbruggen et al. 2007, Li et al. 2008).

The fit of a variety of nucleotide substitution models to the data sets were compared using the second order Akaike information criterion (AICc) (Sullivan and Joyce 2005). Log-likelihoods and AICc scores were calculated for six models of sequence evolution (F81, HKY, and GTR, each with and without among-site rate heterogeneity modeled using the gamma distribution with eight rate classes) and six partitioning strategies (four for the plastid genes and two for the 18S gene) with TreeFinder (Jobb et al. 2004). The AICc scores highlighted the necessity of partitioning the protein data into codon positions and incorporating rate variation among sites (gamma distribution) in the models of sequence evolution (Fig. S3). Models with more substitution categories (e.g., GTR) showed better fit to the data.

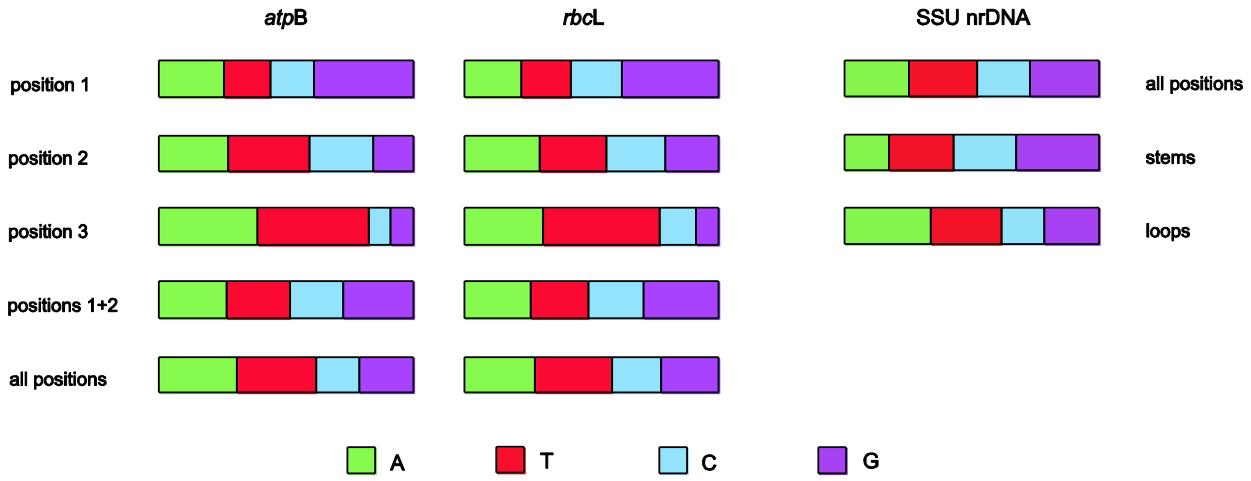

FIG. S1. Base frequencies of potential data partitions. Different codon positions have markedly different base frequencies that deviate from those of combinations of codon positions (positions 1+2 or all positions). The frequencies for individual codon positions barely differ between *atp*B and *rbc*L. Stems and loops of the 18S nrDNA also have different base frequencies, the stems being more GC rich.

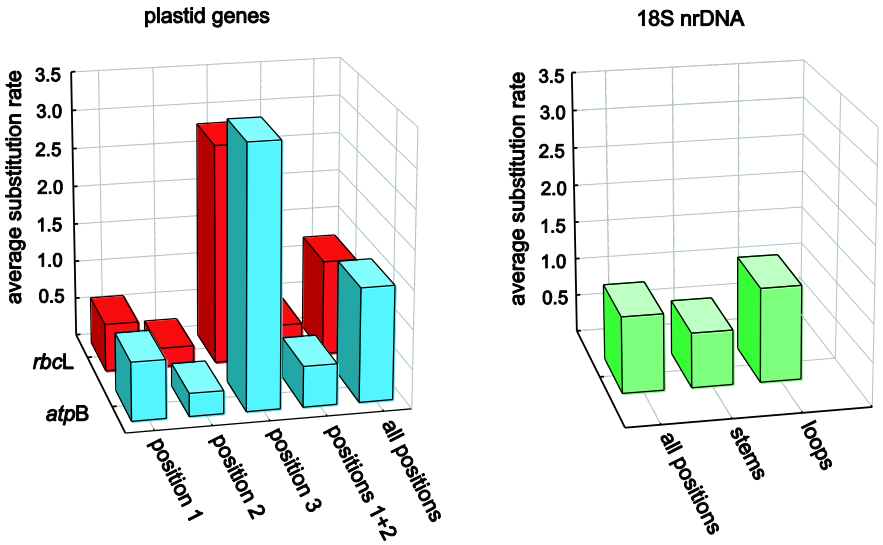

FIG. S2. Average substitution rates of potential data partitions. Both plastid genes show strong rate differences between codon positions that are not well represented in combinations of codon positions (positions 1+2 or all positions). In the 18S nrDNA alignment, stems are somewhat slower than loops.

A – plastid genes

	unpartitioned	genes	codon positions	genes & codon positions

F81	lnL = -54888.6
	# par = 106
	ΔAICc = 21856.1
		lnL = -54889.8
		# par = 110
		ΔAICc = 21867.3
			lnL = -48896.3
			# par = 114
			ΔAICc = 9888.9
				lnL = -48916.4
				# par = 126
				ΔAICc = 9955.4

F81 + Γ_8	lnL = -48025.1
	# par = 107
	ΔAICc = 8131.3
		lnL = -48008.2
		# par = 112
		ΔAICc = 8108.3
			lnL = -46059
			# par = 117
			ΔAICc = 4220.9
				lnL = -46096.2
				# par = 132
				ΔAICc = 4328.2

HKY	lnL = -54622.3
	# par = 107
	ΔAICc = 21325.7
		lnL = -54618.5
		# par = 112
		ΔAICc = 21328.9
			lnL = -48156.9
			# par = 117
			ΔAICc = 8416.7
				lnL = -48131.4
				# par = 132
				ΔAICc = 8398.5

HKY + Γ_8	lnL = -47566.5
	# par = 108
	ΔAICc = 7216.2
		lnL = -47533.7
		# par = 114
		ΔAICc = 7163.8
			lnL = -44684.9
			# par = 120
			ΔAICc = 1479.2
				lnL = -44638.7
				# par = 138
				ΔAICc = 1426.4

GTR	lnL = -52739.4
	# par = 111
	ΔAICc = 17568.5
		lnL = -52738.8
		# par = 120
		ΔAICc = 17587
			lnL = -46994.6
			# par = 129
			ΔAICc = 6118.4
				lnL = -46883.7
				# par = 156
				ΔAICc = 5956.6

GTR + Γ_8	lnL = -46685.6
	# par = 112
	ΔAICc = 5463.1
		lnL = -46649.7
		# par = 122
		ΔAICc = 5413.3
			lnL = -44127.9
			# par = 132
			ΔAICc = 391.7
				lnL = -43898.6
				# par = 162
				ΔAICc = 0

ΔAICc
22000
17600
13200
8800
4400
0

B – 18S nrDNA

	unpartitioned	stem & loop

F81	lnL = -24453.8
	# par = 106
	ΔAICc = 7937.2
		lnL = -24440.2
		# par = 110
		ΔAICc = 7919.1

F81 + Γ_8	lnL = -21234.1
	# par = 107
	ΔAICc = 1500.2
		lnL = -21240.0
		# par = 112
		ΔAICc = 1523.1

HKY	lnL = -23933.4
	# par = 107
	ΔAICc = 6898.8
		lnL = -23859.2
		# par = 112
		ΔAICc = 6761.4

HKY + Γ_8	lnL = -20639.7
	# par = 108
	ΔAICc = 313.6
		lnL = -20565.8
		# par = 114
		ΔAICc = 179.1

GTR	lnL = -23748.0
	# par = 111
	ΔAICc = 6536.8
		lnL = -23599.1
		# par = 120
		ΔAICc = 6259.4

GTR + Γ_8	lnL = -20570.6
	# par = 112
	ΔAICc = 184.3
		lnL = -20467.1
		# par = 122
		ΔAICc = 0

ΔAICc
8000
6400
4800
3200
1600
0

FIG. S3. Fit of different nucleotide substitution models and partitioning strategies to the plastid (A) and 18S nrDNA (B) alignments. Columns represent different partitioning strategies, and rows correspond to nucleotide substitution models. Three main reversible nucleotide substitution models were used: whereas F81 does not distinguish between different substitution types, HKY85 distinguishes between transitions and transversions, and GTR between all six types of substitutions. Among-site rate heterogeneity was ignored or modeled using the gamma distribution with eight rate classes. Each cell displays the log-likelihood of the guide tree under the model in question, the number of parameters of the model, and the AICc scores. The color code represents the AICc score: lower scores (corresponding to greener colors) indicate better fit of the data to the model in question.

REFERENCES

Brandley, M. C., Schmitz, A. & Reeder, T. 2005. Partitioned Bayesian analyses, partition choice, and the phylogenetic relationships of scincid lizards. *Syst. Biol.* 54:373–90.

Guindon, S. & Gascuel, O. 2003. A simple, fast, and accurate algorithm to estimate large phylogenies by maximum likelihood. *Syst. Biol.* 52:696–704.

Jobb, G., von Haeseler, A. & Strimmer, K. 2004. TREEFINDER: a powerful graphical analysis environment for molecular phylogenetics. *BMC Evol. Biol.* 4:18.

Kosakovsky Pond, S. L., Frost, S. D. W. & Muse, S. V. 2005. HyPhy: hypothesis testing using phylogenies. *Bioinformatics* 21:676–9.

Li, C., Lu, G. & Ortí, G. 2008. Optimal data partitioning and a test case for ray-finned fishes (Actinopterygii) based on ten nuclear loci. *Syst. Biol.* 57:519–39.

Sullivan, J. & Joyce, P. 2005. Model selection in phylogenetics. *Annu. Rev. Ecol. Evol. Syst.* 36:445–66.

Swofford, D. L. 2003. *PAUP*: Phylogenetic Analysis Using Parsimony (* and Other Methods).* Sinauer Associates, Sunderland, Massachusetts.

Verbruggen, H., Leliaert, F., Maggs, C. A., Shimada, S., Schils, T., Provan, J., Booth, D., et al. 2007. Species boundaries and phylogenetic relationships within the green algal genus *Codium* (Bryopsidales) based on plastid DNA sequences. *Mol. Phylogenet. Evol.* 44:240–54.

Appendix S2. Supplementary phylogenetic analyses.

Supplementary phylogenetic analyses were performed to evaluate the effect of outgroup selection, removal of fast-evolving sites, alignment method, partitioning strategy, and model selection on tree topology and branch support. Different outgroup combinations were used, including cyanobacterial outgroups for the plastid gene analysis (*Nostoc* and *Trichodesmium*) (Figs. S4, A and B; S5A). To verify the effect of data partitioning, analyses were performed using unpartitioned data sets (Figs. S4, C and D; S5, B and C). Additional analyses were performed with rapidly evolving sites excluded. For the plastid data set, this consisted of excluding the third-codon positions (Fig. S4C); for the 18S data set, the hyper-variable helices E23_1 (65 positions), 43_2 (26 positions), and 49_2 (42 positions) [see Van de Peer et al. (1999) for RNA secondary structure nomenclature] were removed (Fig. S5D). Because alignment of the 18S sequences was notoriously difficult, we also aligned this data set using MUSCLE (Edgar 2004) to assess the effect of alignment method on phylogenetic reconstruction. The MUSCLE alignment was analyzed with and without divergent and ambiguously aligned regions removed with Gblocks (Castresana 2000) (alignments 1,717 and 1,956 bases long, respectively) (Fig. S5D). Since about half of the 18S alignment consisted of invariant position, we also analyzed the 18S data sets (MUSCLE and secondary structure based alignment, with and without removal of divergent regions) using a single partition and a GTR+Γ_4+I model, but this had no effect on tree topology (data not shown).

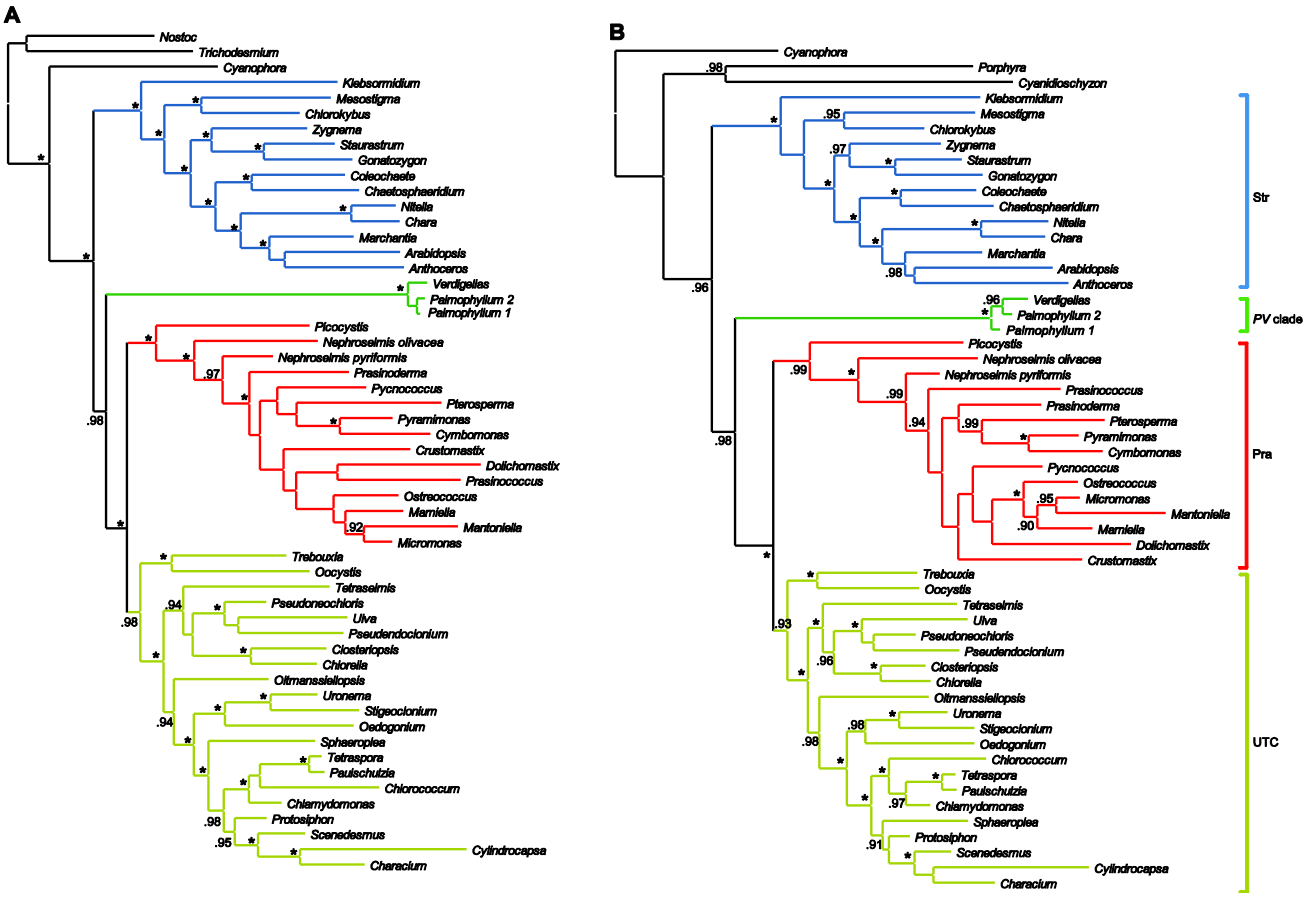

FIG. S4. Trees obtained from Bayesian analyses of the plastid genes. Values given at nodes are posterior probabilities (values <0.9 are not shown); the nodes that received full support are denoted by an asterisk. (A–B) Analyses with alternative outgroup combination. (A) The cyanobacteria *Nostoc* and *Trichodesmium* were used as outgroups in addition to *Cyanophora*. (B) The red algae *Pophyra* and *Cyanidioschyzon* were used as outgroups in addition to *Cyanophora*.

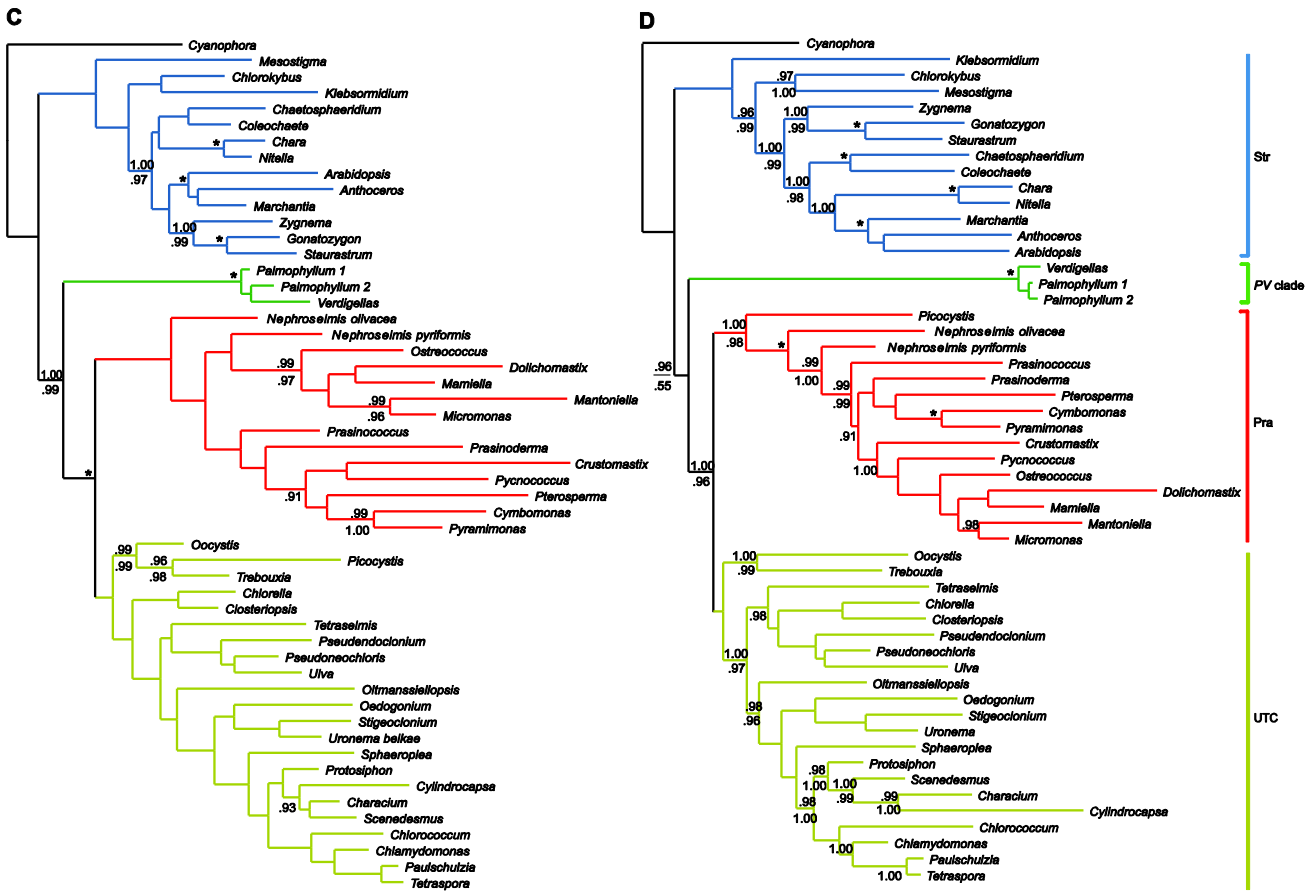

FIG. S4 (continued). Trees obtained from Bayesian analyses of the plastid genes. (C–D) Analyses based on data sets with third codon positions ex- or included. (C) Analyses performed on a data set with first two codon positions only, with the data set partitioned into codon positions and a GTR+Γ8 model selected for each partition (posterior probabilities above branches), and analysis under a single partition with a GTR+Γ8 model selected (posterior probabilities below branches). (D) Analysis of the full data set (all three codon positions) with the data set partitioned into codon positions and a GTR+Γ8 model selected for each partition (= Fig. 2A of main paper, posterior probabilities above branches), and analysis under a single partition with a GTR+Γ8 model selected (posterior probabilities below branches).

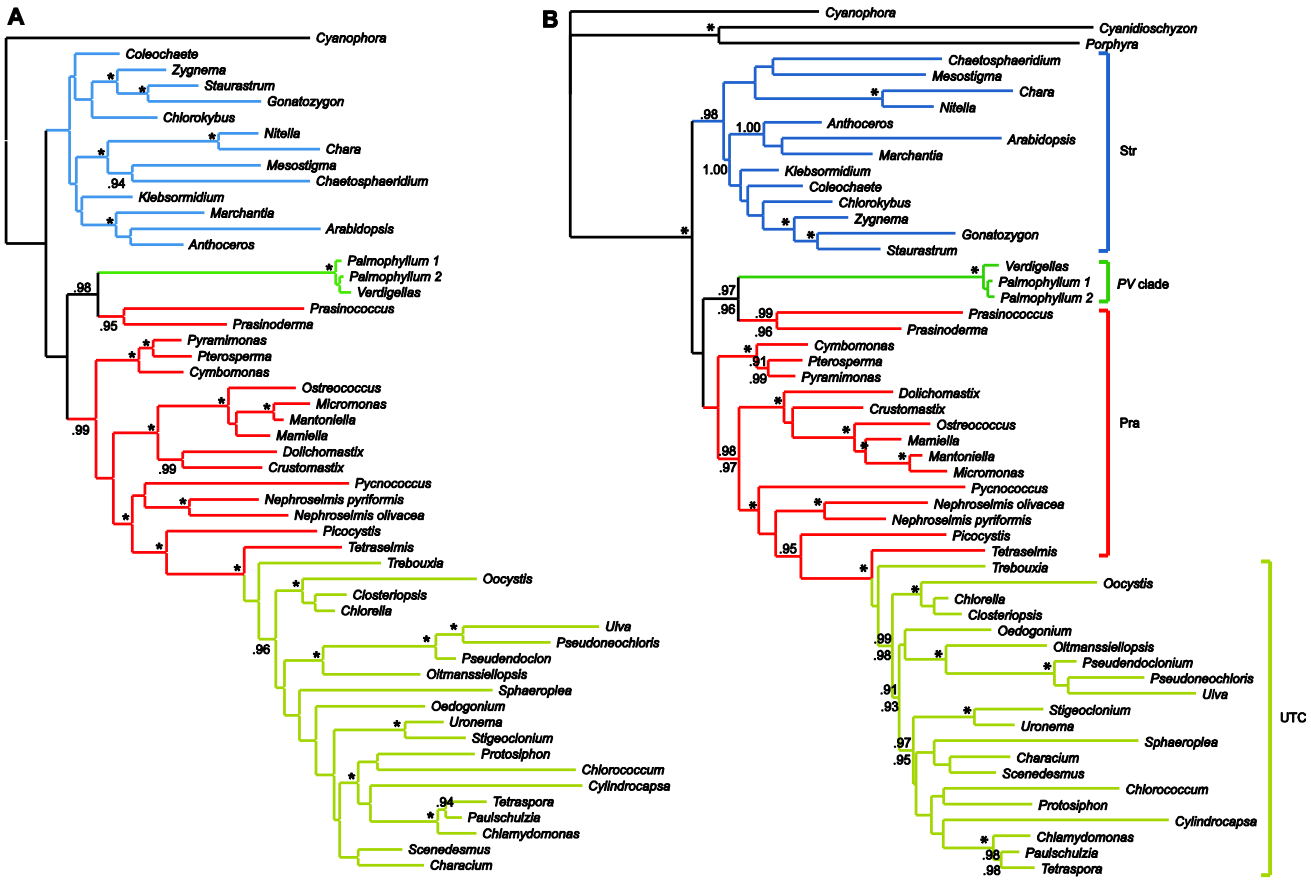

FIG. S5. Trees obtained from Bayesian analyses of the 18S nrDNA alignment. Values given at nodes are posterior probabilities; values below 0.9 are not shown; the nodes that received full support are denoted by an asterisk. (A) Phylogeny inferred from the complete RNA secondary structure based alignment (2,000 positions) with only *Cyanophora* as the outgroup. (B) Phylogeny inferred from the RNA secondary structure based alignment with variable helices removed (1,867 positions included), with the data set partitioned into stems and loops and a GTR+Γ8 model selected for each partition (posterior probabilities above branches), and analysis under a single partition with a GTR+Γ8 or GTR+Γ4+I model selected (posterior probabilities below branches).

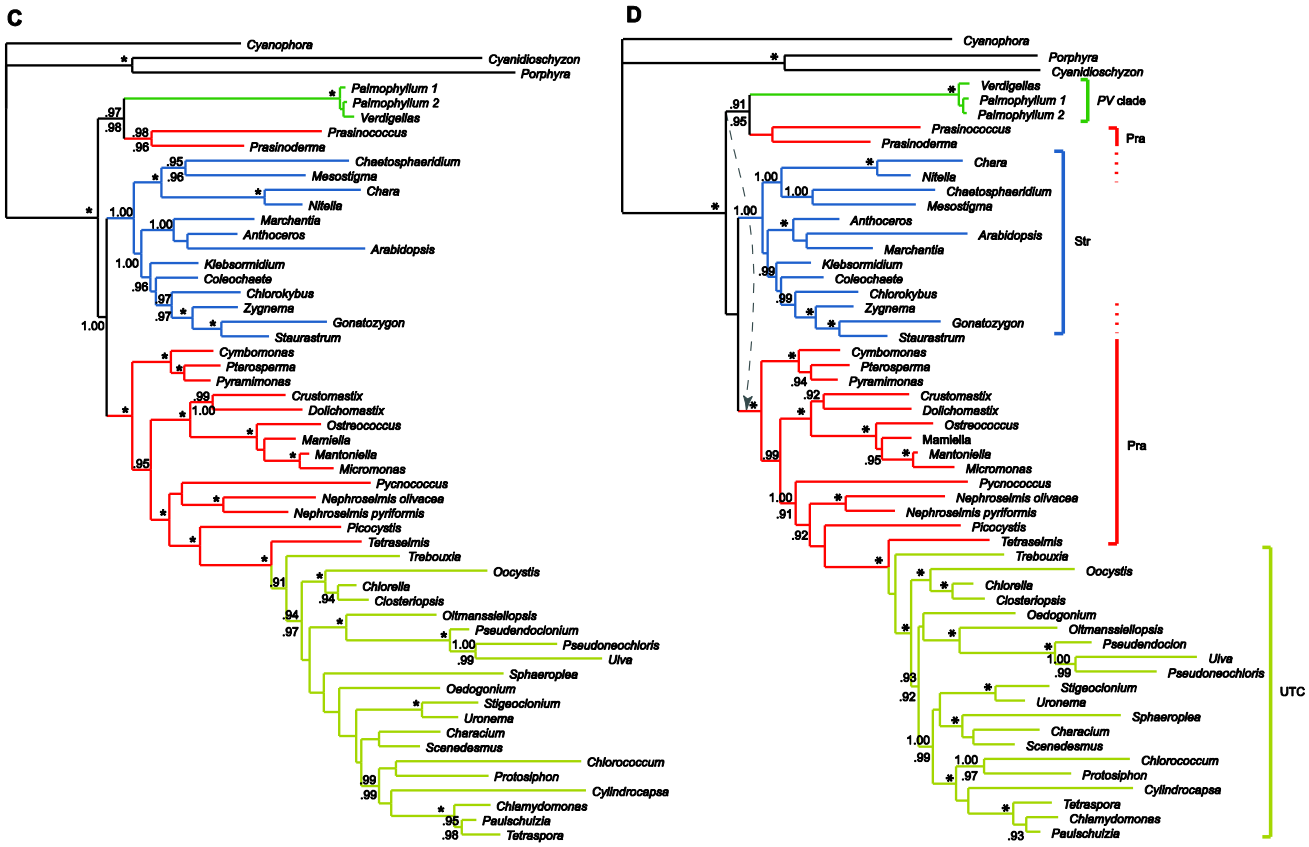

FIG. S5 (continued). Trees obtained from Bayesian analyses of the 18S nrDNA alignment. (C) Phylogeny inferred from the complete RNA secondary structure based alignment (2,000 positions), with the data set partitioned into stems and loops and a GTR+Γ8 model selected for each partition (= Fig. 2B of main paper, posterior probabilities above branches), and analysis under a single partition with a GTR+Γ8 model selected (posterior probabilities below branches). (D) Phylogeny inferred from the MUSCLE alignment with a single partition under a GTR+Γ8 model; analyses were performed using the complete alignment (1,956 positions, posterior probabilities above branches) or an alignment with poorly aligned positions excluded with Gblocks (1,717 positions, posterior probabilities below branches); the arrow indicates the position of the *PV-Prasinococcus-Prasinoderma* clade in the latter analysis (posterior probability 0.54).

REFERENCES

Castresana, J. 2000. Selection of conserved blocks from multiple alignments for their use in phylogenetic analysis. *Mol. Biol. Evol.* 17:540–52.

Edgar, R. C. 2004. MUSCLE: a multiple sequence alignment method with reduced time and space complexity. *BMC Bioinformatics* 5:1–19.

Van de Peer, Y., Robbrecht, E., de Hoog, S., Caers, A., De Rijk, P. & De Wachter, R. 1999. Database on the structure of small subunit ribosomal RNA. *Nucleic Acids Res.* 27:179–83.

Table S1. List of taxa used in this study, with GenBank accession numbers of their *atp*B and *rbc*L and 18S nrDNA sequences. In some cases, genes from different species of the same genus were concatenated if the monophyly of the genus had been clearly demonstrated. New sequences are indicated in bold.

	*atp*B	*rbc*L	18S nrDNA
Chlorophyta			
Ulvophyceae			
Ulotrichales			
Pseudoneochloris marina S. Watanabe et al. 2000		AF499682	U41102
Pseudendoclonium akinetum Tupa	NC_008114	NC_008114	DQ011230
Ulvales			
Ulva intestinalis Linnaeus		AY422552	AJ000040
uncertain affinities			
Oltmannsiellopsis viridis (Hargraves et Steele) Chihara et Inouye	NC_008099	NC_008099	D86495
Trebouxiophyceae			
Chlorellales			
Chlorella vulgaris Beijerinck	NC_001865	NC_001865	X13688
Closteriopsis acicularis (G. M. Smith) Belcher et Swale	EF113502	EF113433	Y17470
Oocystales			
Oocystis apiculata West	EF113524	EF113549	AF228686 *O. solitaria*
Trebouxiales			
Trebouxia magna Archibald	EF113541	AJ969630	Z21552
Chlorophyceae			
Chaetophorales			
Stigeoclonium helveticum Vische	NC_008372	NC_008372	U83131
Uronema belkae G. M. Lokhorst	EF113544	EF113481	AF182821
Chlamydomonadales/Volvocales			
Chlamydomonas reinhardtii P. A. Dangeard	NC_005353	NC_005353	M32703
Chlorococcum echinozygotum Starr	EF113500	EF113430	U57698
Protosiphon botryoides G. A. Klebs		EF113465	U41177
Oedogoniales			
Oedogonium cardiacum (Hassall) Wittrock	EF113523	EF113458	U83133
Sphaeropleales			
Scenedesmus obliquus (Turpin) Kützing	NC008101	NC008101	AJ249515
Sphaeroplea robusta M. A. Buchheim et L. R. Hoffman	EF113536	EF113472	U73472
Tetrasporales			
Paulschulzia pseudovolvox (Schultz) Skuja	AB014040	D86837	U83120
Tetraspora sp. Link	EF113540	EF113477	U83121
uncertain affinities			
Cylindrocapsa geminella Wolle	EF119849	EF113434	AF387159
Prasinophyceae			
Chlorodendrales			
Tetraselmis suecica (Kylin) Butcher	DQ173248	DQ173247	X70802 *T. striata*
Mamiellales			
Crustomastix stigmatica Zingone		AF509626	AF509628
Dolichomastix tenuilepis J. Throndsen et A. Zingone		AF509627	AF509625
Mamiella sp. Ø. Moestrup		U30277	AB017129
Mantoniella squamata (I. Manton et M. Parke) T. V. Desikachary		U30278	X73999
Micromonas pusilla (R. W. Butcher) I. Manton et M. Parke		AY955031	AY954994
Ostreococcus tauri C. Courties et M.-J. Chrétiennot-Dinet	NC_008289	NC_008289	AY329635
Prasinococcales			
Prasinococcus sp. H. Miyashita et M. Chihara		EU449501	AF203400
Prasinoderma coloniale T. Hasegawa et M. Chihara		EU449500	AB058379
Pseudoscourfieldiales			
Pycnococcus provasolii R. R. L. Guillard		U30280	X91264
Pyramimonadales			
Cymbomonas tetramitiformis Schiller		L34687	AB017126
Nephroselmis olivacea F. Stein	NC_00927	NC_00927	X74754
Nephroselmis pyriformis (N. Carter) Ettl		EU449502	X75565
Pterosperma cristatum Schiller		U30281	AB017127
Pyramimonas disomata Butcher ex McFadden, Hill et Wetherbee			AB017121
Pyramimonas olivacea N. Carter		L34815	AB017122
uncertain affinities			
Picocystis salinarum R. A. Lewin		AF528186	AF153313
Palmophyllales			
Palmophyllum umbracola.1 W. A. Nelson et K. G. Ryan	**EU580405**	**EU586180**	**FJ619275**
Palmophyllum umbracola.2	**EU586181**	**EU586182**	**FJ619276**
Verdigellas peltata D. L. Ballantine et J. N. Norris		**EU586183**	**FJ619277**
Streptophyta			
Charophyceae			
Charales			
Chara connivens Salzmann ex A. Braun	AF408782	L13476	U18493
Nitella flexilis (Linnaeus) C. Agardh	AB110837	AB076056	U05261
Klebsormidiophyceae			
Coleochaetales			
Coleochaete scutata Brébisson 1844	AY082303	AY082313	X68825
Klebsormidiales			
Chlorokybus atmophyticus Geitler	DQ422812	DQ422812	M95612
Klebsormidium flaccidum (Kützing) P. C. Silva, K. Mattox et W. Blackwell	AF408801	AF408253 *K. subtilissimum*	X75520
Chaetosphaeridiales			
Chaetosphaeridium globosum (Nordstedt) Klebahn	NC_004115	NC_004115	AF113506
Mesostigmatophyceae			
Mesostigmatales			
Mesostigma viride Lauterborn	NC_002186	NC_002186	AJ250109
Zygnematophyceae			
Zygnematales			
Gonatozygon monotaenium De Bary	AF408796	U71438	X91346 *G aculeatum*
Staurastrum punctulatum Brébisson ex Ralfs	NC_008116	NC_008116	AF115442
Zygnema circumcarin Czurda	NC_008117	NC_008117	AJ853450 *Z. pseudogedeanum*
Marchantiopsida			
Marchantiales			
Marchantia polymorpha Linnaeus	NC_001319	NC_001319	AB021684
Anthoceratopsida			
Anthocerotales			
Anthoceros formosae Steph.	NC_004543	NC_004543	X80984 *A. agrestis*
spermatophytes			
Brassicales			
Arabidopsis thaliana (L.) Heynh.	NC_000932	NC_000932	AC006837